Seismic Effect of Height Fluid Filling on Storage Cylindrical Container

KAMILA KOTRASOVÁ, EVA KORMANÍKOVÁ
Department of Structural Mechanics, Institute of Structural Engineering, Faculty of Civil Engineering
The Technical University of Košice
Vysokoškolská 4, 042 00 Košice
SLOVAK REPUBLIC
kamila.kotrasova@tuke.sk, eva.kormanikova@tuke.sk

Abstract: - Liquid storage cylindrical containers are built for storing a variety of liquids. The seismic behavior of tanks is, however, quite complex problem. The interaction of tank and liquid can be simplified with the concept of generalized single-degree-of-freedom systems representing the convective, rigid impulsive and flexible impulsive vibration modes. This paper presents the theoretical background for cylindrical tanks fixed to rigid foundation under earthquake loading, describing the fluid hydrodynamic pressure and the seismic response of liquid storage tank. The base shears, the bending moment and overturning moment are calculated by using the response spectra for risk region of Slovakia, B category of subsoil. The seismic analysis was made on the ground supported cylindrical concrete tanks with considering of partial fulfillments.

Key-Words: - Container, fluid, earthquake, pressure, shear, moment.

1 Introduction

Ground-supported liquid storage containers are built for storing a variety of liquids, e.g. water for drinking and fire-fighting, petroleum, oil, liquefied natural gas, chemical fluids, chemical and radioactive fluid wastes. Liquid storage reservoirs are strategically very important structures, since they have vital uses in industries, nuclear power plants and are connected to public life. Seismic safely of liquid tanks is of considerable importance [1-7, 10]. Water storage tanks should remain functional in the post-earthquake period to ensure potable water supply to earthquake-affected regions and to cater the need for fighting demand. Industrial liquid tanks containing highly toxic and inflammable liquids and these tanks should not lose their contents during the earthquake. Satisfactory performance of tanks during strong ground shaking is crucial for their modern facilities. The seismic behavior of liquid storage containers is highly complex problem due to liquid-structure interaction [9, 13-19].

Seismic analysis of liquid-containing tanks is different from analysis of structures. The fluid, inside of the thanks, is exerted hydrodynamic effects on tank wall and base. The knowledge of liquid hydrodynamic pressures, forces and seismic effects developed during an earthquake are importance for secure design of containers [11, 20-22].

As first probably, Westergaard (1933) determined the pressures on a rectangular dam subjected to horizontal acceleration. Jacobsen analyzed a rigid cylindrical liquid-containing tank and cylindrical pier surrounded by liquid, subjected to horizontal acceleration (1949, 1951). Housner (1963) obtained the expressions for distribution of hydrodynamic pressure on a rigid tank wall due to lateral base excitation with considering of two components, impulsive and convective, of hydrodynamic pressure. Veletsos (1984) presented the distribution of hydrodynamic pressure on rigid with and also flexible wall.

Housner [4] simplified the method of hydrodynamic analysis of system tank-liquid and introduced the concept of two dynamic components. The Housner established dynamic impulsive and convective masses simulate the impulsive and convective mode of vibration of tank-fluid system. Housner's spring-mass system modified Graham with Rodriquez (1952) and Epstein (1976). Velestos and Yang (1977) presented a different approach to arrive for mechanical model of circular rigid tanks. Haround with Housner (1981) and Velestos (1984) analyzed mechanical model for flexible containers. Malhotra Wenk, Wieland [12] simplified the Velestos flexible cylindrical model and studied the dynamic behavior of unanchored and base-isolated liquid cylindrical storage tanks [6].

The seismic design of cylindrical liquid storage tanks is recommended by various standards, e.g. Eurocode 8, ACI 350.3, AWWA standards, API 650, NZSEE guidelines and Indian code IS 1893-1984 [24].

European Committee for Standardization prepared code Eurocode 8 (2006). Part 4 [23] of this

code recommended seismic design of liquid storage tanks, silos and pipelines. Eurocode 8 use Velestos's hydrodynamic pressure distribution in cylindrical containers, Veletsos and Yang mechanical model as an acceptable procedure for rigid cylindrical reservoirs. Haroun and Housner and as well as Veletsos models are recommended together with the simplified procedure of Malhotra, Wenk, Wieland [12] for flexible cylindrical containers.

2 Seismically induced hydrodynamic pressure components of liquid filled tank

The motion of the fluid contained in a rigid shell may by expressed as the sum of two separate contributions, which called "rigid" impulsive and convective, respectively. The "rigid" impulsive component satisfies exactly the boundary conditions at the walls and the bottom of the tank, but gives (incorrectly, due to the presence of the waves in the dynamic response) zero pressure at the original position of the free surface of the fluid in the static situation. The "convective" term does not alter those boundary conditions that are already satisfied, while fulfilling the correct equilibrium condition at the free surface [23].
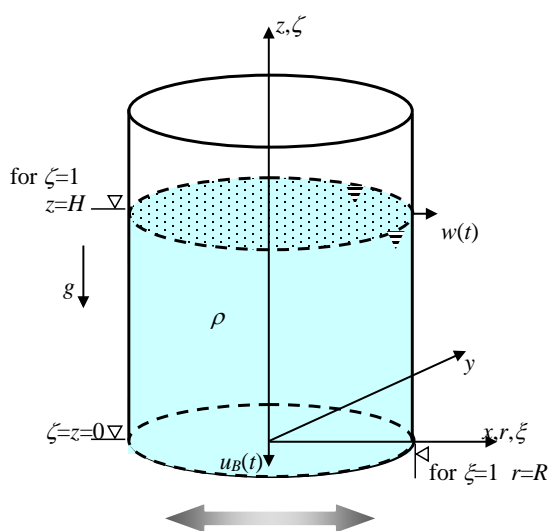

Fig. 1. Cylindrical tank

The seismic load acting on wall and bottom of cylindrical container (Fig. 1) the following pressure components:

- the impulsive "rigid" pressure component,
- the convective pressure component,
- the impulsive "flexible" pressure component.

The impulsive "rigid" pressure component caused by inertia of the liquid, when the rigid tank moves together with the foundation.

The convective pressure component presents phenomenon when liquid vibrates, it shows as well as sloshing.

The impulsive "flexible" pressure component caused by the combined vibration of the flexible container with liquid, when the tank (e.g. steel tanks) doesn't move together with the foundation.

2.1 Rigid impulsive component

Use is made of a cylindrical coordinate system in Fig. 1: r, z, θ, with origin at the center of the tank bottom. R is the tank radius in [m], H is high of fluid filing in [m], ρ is the fluid mass density, while $\xi = r/R$ is non-dimensional radius and $\zeta = z/H$ is non-dimensional coordinate.

The spatial-temporal variation of the "rigid" impulsive pressure is given by the expression

$$p_i(\xi, \zeta, \theta, t) = C_i(\xi, \zeta)\rho H \cos\theta A_g(t), \qquad (1)$$

where

$$C_i(\xi, \zeta) = 2\sum_{n=0}^{\infty} \frac{(-1)^n}{I_1'(\nu_n/\gamma)\nu_n^2} \cos(\nu_n\zeta) I_1\left(\frac{\nu_n}{\gamma}\xi\right), \quad (2)$$

$\nu_n = \pi\dfrac{2n+1}{2}$ and $\gamma = H/R$. $I_1\left(\dfrac{\nu_n}{\gamma}\xi\right)$ is the

modified Bessel function of order 1 and $I_1'\left(\dfrac{\nu_n}{\gamma}\xi\right)$ is

derivate can be expressed in terms of modified Bessel function of order 0 and 1

$I_1\left(\dfrac{\nu_n}{\gamma}\xi\right) = I_0\left(\dfrac{\nu_n}{\gamma}\xi\right) - \dfrac{I_1\left(\dfrac{\nu_n}{\gamma}\xi\right)}{\dfrac{\nu_n}{\gamma}\xi}$. The function C_i

gives the distribution along the height of p_i. θ is angle of circumference, $\gamma = H/R$ is tank slenderness parameter, $A_g(t)$ is the horizontal ground acceleration time-history in free-field with peak value denoted by a_g as a result of an equivalent single-degree-of-freedom system with a impulsive period T_i.

Figure 2 shows the mode of vibration. Figures 3 and 4 present:

- the schematic distribution of impulsive "rigid" pressure component, when pressures considered only on the tank wall and resultant of the impulsive "rigid" pressure component on the wall (Fig. 3),

- the schematic distribution of impulsive "rigid" pressure component, when pressures considered on the tank wall and bottom together, resultant of the impulsive "rigid" pressure component on the wall and bottom (Fig. 4).
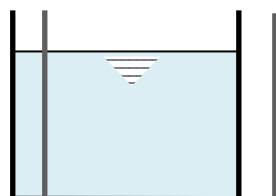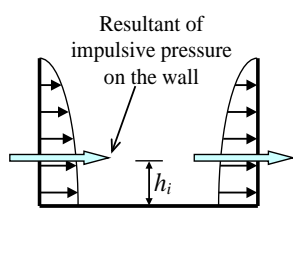

Fig. 2. Mode of vibration

Fig. 3. Distribution of the impulsive pressure and resultant only on the wall
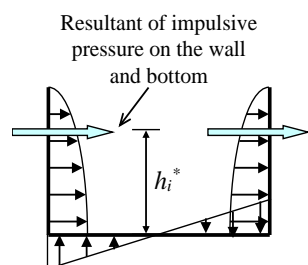
Fig. 4. Distribution of the impulsive pressure and resultant on the wall and bottom

2.2 Convective pressure component

The spatial-temporal variation of the convective pressure component is given

$$p_c(\xi,\zeta,\theta,t) =$$
$$= \rho \sum_{n=1}^{\infty} \psi_n \cos(\nu_n \gamma \zeta) J_1(\nu_n \xi) \cos \theta A_{cn}(t), \quad (3)$$

where

$$\psi_n = \frac{2R}{(\lambda_n^2 - 1) J_1(\lambda_n) \cosh(\lambda_n \gamma)} \quad (4)$$

J_1 is Bessel function of the first order, λ_n are the roots of the first-order Bessel function of the first kind ($\lambda_1 = 1.8412$; $\lambda_2 = 5.3314$; $\lambda_3 = 8.5363$, $\lambda_4 = 11.71$, $\lambda_5 = 14.66$ and $\lambda_{5+i} = \lambda_5 + 5 \cdot i$ for i is given 1,2,...). $A_{cn}(t)$ is acceleration time-history of the response of a single degree of freedom oscillator having a circular frequency ω_{cn} given by

$$\omega_{cn} = \sqrt{\frac{g \lambda_n \tanh(\lambda_n \gamma)}{R}}, \quad (5)$$

so

$$T_{cn} = \frac{2\pi}{\sqrt{\dfrac{g \lambda_n \tanh(\lambda_n \gamma)}{R}}} \quad (6)$$

and a 0.5% damping ratio appropriate for the sloshing of the fluid.

Only the first oscillating (sloshing) mode and frequency of the oscillating liquid ($n=1$) needs to be considered in expression for design purposes.

$$\omega_{c1} = 4.2 / \sqrt{R} \quad (7)$$

which, for the usual values of R yields periods of oscillation of the order of few seconds.

Only the first convective mode of vibration needs to be considered for practical applications in the analysis.

The mode of vibration is shown in Figure 5. Figures 6 and 7 document:

- the schematic distribution of convective pressure component, when pressures considered only on the tank wall and resultant of the convective pressure component on the wall (Fig. 6),
- the schematic distribution of convective pressure component, when pressures considered on the tank wall and bottom together, resultant of the convective pressure component on the wall and bottom (Fig. 7).
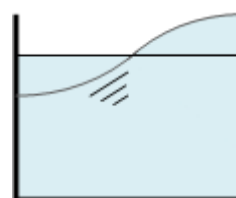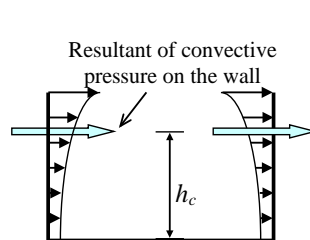

Fig. 5. Mode of vibration

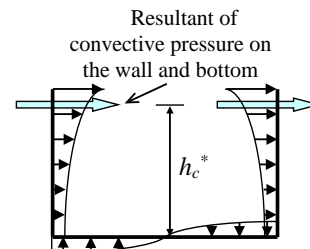Fig. 6. Distribution of the convective pressure and resultant only on the wall

Fig. 7. Distribution of the convective pressure and resultant on the wall and bottom

2.3 Flexible impulsive component

It is normally unconservative to consider the tank as rigid. In flexible tanks the fluid pressure is usually expressed as the sum of tree contributions, referred to as: "rigid" impulsive, convective (sloshing) and "flexible" impulsive. The third satisfied the condition that the radial velocity of the fluid along the wall equals the deformation velocity of the tank wall, as well as the conditions of zero vertical velocity at the tank bottom and zero pressure at the free surface of the fluid. The dynamic coupling between the sloshing and the flexible components is very weak, due to the large differences between the frequencies of the sloshing motion and of the deformation of the wall, which allows determining the third component independently of the others.

The flexible pressure distribution depends on the modes of vibration of tank fluid system, among which those one circumferential wave, of the following type, are of interest

$$\phi(\zeta, \theta) = f(\zeta)\cos\theta \qquad (8)$$

The radial distribution of the flexible impulsive pressure on the tank bottom is qualitatively the same as for the rigid impulsive pressure. Assuming the modes as known, the flexible pressure distribution on the walls has the form

$$p_f(\zeta, \theta, t) = \rho H \psi \cos\theta \sum_{n=1}^{\infty} \cos(\nu_n \zeta) A_{fn}(t) \qquad (9)$$

where

$$\psi = \frac{\int_0^1 f(\zeta)\left[\dfrac{\rho_s}{\rho}\dfrac{s(\zeta)}{H} + \sum_{n=1}^{\infty} b_n' \cos(\nu_n \zeta)\right]d\zeta}{\int_0^1 f(\zeta)\left[\dfrac{\rho_s}{\rho}\dfrac{s(\zeta)}{H}f(\zeta) + \sum_{n=1}^{\infty} d_n \cos(\nu_n \zeta)\right]d\zeta}, \qquad (10)$$

$$b_n' = 2\frac{(-1)^n I_1(\nu_n/\gamma)}{\nu_n^2 I_1'(\nu_n/\gamma)} \qquad (11)$$

and

$$d_n = 2\frac{\int_0^1 f(\zeta)\cos(\nu_n \zeta)d\zeta\, I_1(\nu_n/\gamma)}{\nu_n I_1' \cos(\nu_n \zeta)}, \qquad (12)$$

ρ_s is the mass density of the shell, $s(\zeta)$ is its thickness and $A_{fn}(t)$ is the response acceleration (relative to its base) of a simple oscilator having the period and damping ratio of mode n. The fundamental mode ($n=1$) is normally sufficient, so that in expressions (9), (11), (12), the mode index, n, and the summation over all modal contributions are dropped.

The fundamental circular frequency of the tank-fluid system may be evaluuated by means of the following approximate expression

$$\omega_f = 2\pi\frac{\sqrt{E\,s(\zeta)/\rho H}}{2R(0,157\gamma^2 + \gamma + 1,49)}, \qquad (13)$$

E is elastic modulus of the material of the tank wall.

Figure 8 shows the mode of vibration. Figures 9 and 10 present:

- the distribution of flexible impulsive pressure component, when pressures considered only on the tank wall and resultant of the convective pressure component on the wall (Fig. 9),
- the distribution of flexible impulsive pressure component, when pressures considered on the tank wall and bottom together, resultant of the convective pressure component on the wall and bottom (Fig. 10).
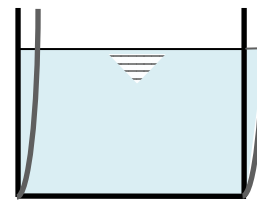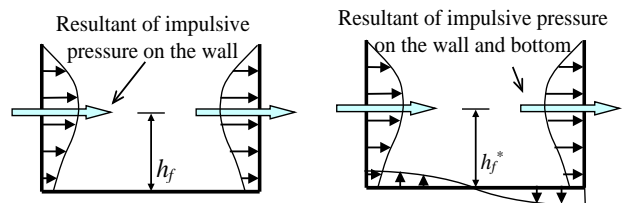

Fig. 8. Mode of vibration

| Fig. 9. Distribution of the flexible impulsive e pressure and resultant only on the wall | Fig. 10. Distribution of the flexible impulsive pressure and resultant on the wall and bottom |

3 Mechanical model for fixed base cylindrical fluid filled tank

The dynamic analysis of the tank-liquid system may be modelled by two single - degree of freedom (SDOF) systems, one corresponding to the impulsive component, moving together with the flexible wall, and the others corresponding to the convective components for n - mode of vibration, see Figure 11. The impulsive and convective responses are combined by taking their numerical sum.
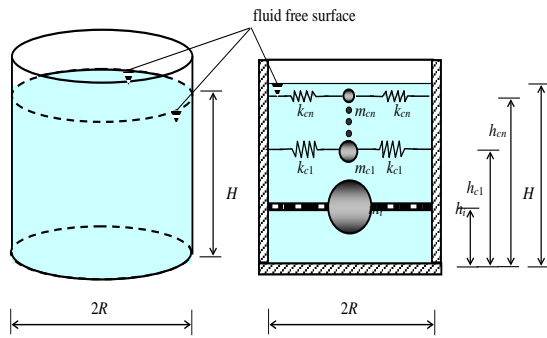
Fig. 11. Liquid-filled tank modelled by generalized single degree of freedom systems.

The presented simple procedure for seismic analysis of liquid-storage tanks [12] was used in Eurocode 8 [23].

For a ground supported cylindrical tank, in which the wall is rigidly connected with the base slab, time period of impulse mode of vibration T_i in [s] is given by

$$T_i = C_i \frac{H\sqrt{\rho}}{\sqrt{s/R}\sqrt{E}}, \qquad (14)$$

and

$$T_c = C_c \sqrt{R}, \qquad (15)$$

where C_i is coefficient of time period for impulsive mode witch is dimensionless and C_c is coefficient of time period for convective mode in [s/m$^{1/2}$]. The values of C_i, C_c are given from Figure 12 as function of the tank slenderness parameter $\gamma = H/R$.
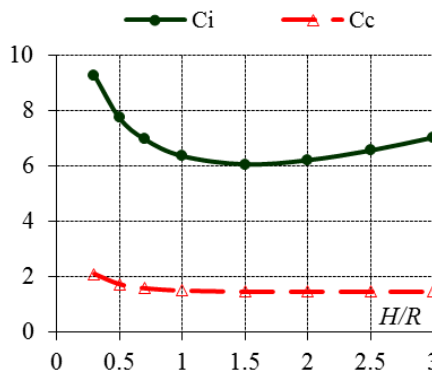

Fig. 12. Coefficients C_i and C_c as function of the tank slenderness parameter $\gamma = H/R$

H and R are tank's height and radius of fluid filling, s is equivalent uniform thickness of the wall (weighted average over the wetted height of the wall, the weight may be taken proportional to the

strain in the wall of the tank, which is maximum at the base of the tank), ρ is mass density of liquid and E is tank material modulus of elasticity.
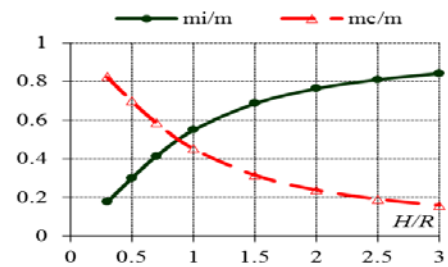

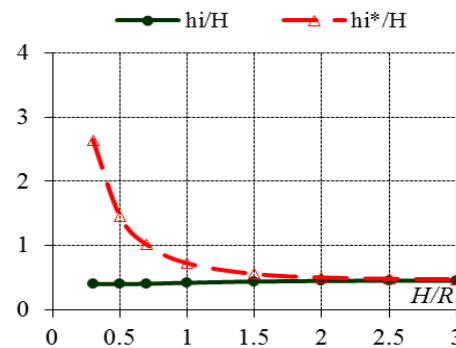Fig. 13. Ratios m_i/m and m_c/m as function of the tank slenderness parameter $\gamma = H/R$.

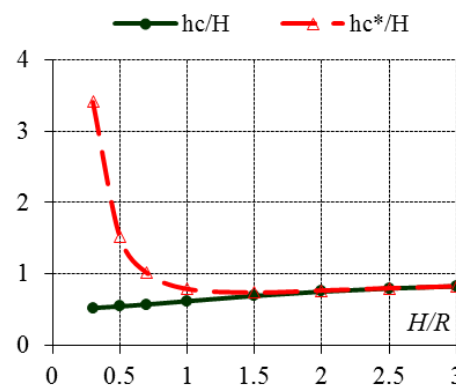Fig. 14. Ratios h_i/H and h_i^*/H as functions of the parameter tank slenderness $\gamma = H/R$.

Fig. 15. Ratios h_c/H and h_c^*/H as functions of the tank slenderness parameter $\gamma = H/R$.

The values of the impulsive and convective masses m_i and m_c as fraction of the total liquid mass m are shown in Figure 13 as function of the tank slenderness parameter $\gamma = H/R$.

The values of the corresponding heights from the base of the point of application of the resultant of the impulsive and convective hydrodynamic wall pressure as fraction as function of the fluid filling H. h_i, h_c are documented in Fig. 14 and h_i^*, h_c^* in Fig. 15 as function of the tank slenderness parameter $\gamma = H/R$.

Seismic response: the total base shears and moments of ground supported tank can be obtained by combining the overturning moment in impulsive and convective mode:

- the total base shear at the bottom of the wall

$$V = (m_i + m_w + m_r)S_e(T_i) + (m_c)S_e(T_c), \quad (16)$$

- the total base shear at the bottom of base slab

$$V^* = (m_i + m_w + m_b + m_r)S_e(T_i) + (m_c)S_e(T_c), \quad (17)$$

- The overturning moment immediately above the base plate

$$M = (m_i h_i + m_w h_w + m_r h_r)S_e(T_i) + (m_c h_c)S_e(T_c), \quad (18)$$

- The overturning moment immediately bellow the base plate

$$M^* = (m_i h_i^* + m_w h_w^* + m_r h_r^* + m_b(t_b/2))S_e(T_i) + \\ + (m_c h_c^*)S_e(T_c), \quad (19)$$

where m_w is mass of tank wall, m_b is mass of base slab and m_r is mass of roof of tank. Spectral acceleration, obtained from an elastic response spectrum $S_e(T)$ will be calculated separately for impulsive $S_e(T_i)$ and convective mode $S_e(T_c)$. The impulsive Spectral acceleration is obtained from 2 % damped elastic response spectrum for steel or pre-stressed concrete tanks and 5 % damped elastic response spectrum for concrete and masonry tanks. The convective Spectral acceleration is obtained from 0.5 % damped elastic response spectrum [23].

4 Numerical example and results

The ground supported concrete cylindrical reservoir has inner diameter $D = 20$ m and height H 10 m. Tank wall has uniform thickness $s = 0.6$ m. The base slab thick d is 0.6 m with diameter 20.9 m. Container is without roof slab. Tank is made from concrete, therefore, $E = 3.40 \cdot 10^7$ kNm^{-2} and $\rho = 2{,}540$ kg/m^3. The reservoir is filled with water (H$_2$O, density $\rho_w = 1{,}000$ kg/m^3) to maximal height 10 m. We consider only horizontal seismic load. The elastic response spectrum was used for Slovakia region with $a_g = 1.5$ ms^{-2} B category of subsoil. The

impulsive spectral accelerations are obtained from a 5% damped elastic response spectrum (for concrete tanks) and the convective spectral accelerations are obtained from a 0.5% damped elastic response spectrum.

A ground supported concrete cylindrical tank has capacity 3000 m^3. We considered different height of fluid filling: empty tank, heights of tank fluid filling are 1 m, 2 m, 3 m, 4 m, 5 m, 6 m, 7 m, 8 m, 9 m and theoretically 10 m. The tank slenderness parameter given is by relation $\gamma = H/L$. In this cases the tank slenderness parameters are 0.1, 0.2, 0.3, 0.4, 0.5, 0.6, 0.7, 0.8, 0.9 and 1.0.
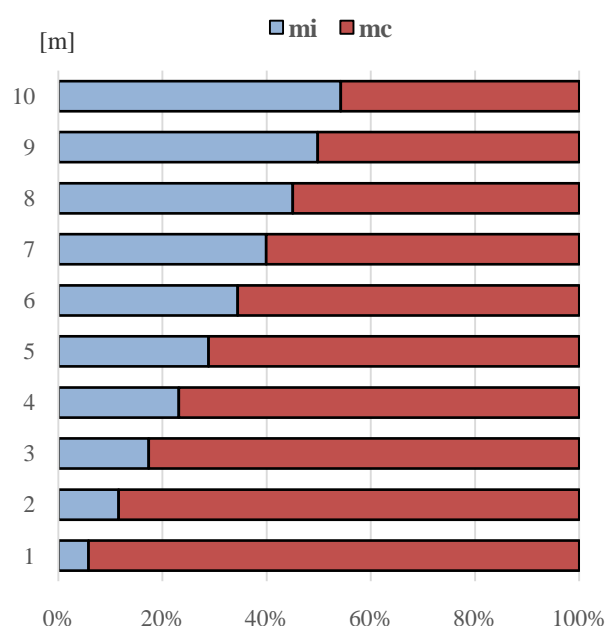

Fig. 16. Comparison of the mass (impulsive and convective) components of the fluid contained in tank as functions of the tank fluid filling
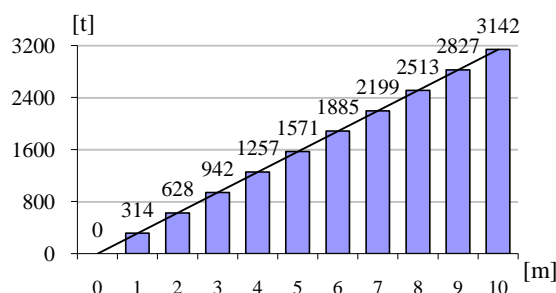

Fig. 17. The total mass of contained fluid as function of the tank fluid filling

Figure 16 shows comparison of component ratio of the impulsive mass m_i and the convective mass m_c as fraction of the total liquid mass m in depended on the tank fluid filling. It is seen, that with height

fluid filling of tank m_i is growing. If the tank is little filled only, then almost all of the fluid has a convective effect. The total mas of contained fluid as function of the tank fluid filling is shown in Figure 17, the grooving total mas function has linear tendency.

Figure 18 presents the comparison of the base shears at the bottom of the wall in impulsive and convective mode of fluid as function of the tank fluid filling. It is seen that value of the base shears in impulsive mode of fluid are grooving notable with height of tank fluid filling. Figure 19 documents the comparison of the base shears of tank wall and tank bottom also as function of the tank fluid filling.
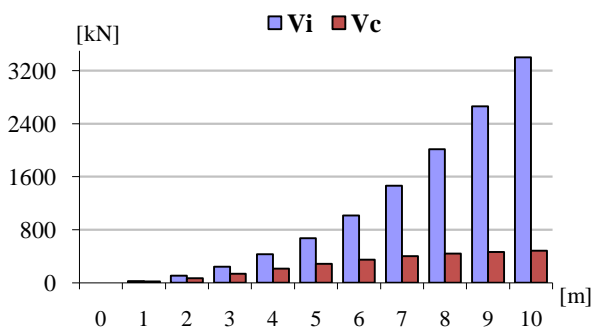

Fig. 18. Comparison of the base shears in impulsive and convective mode of fluid as function of the tank fluid filling
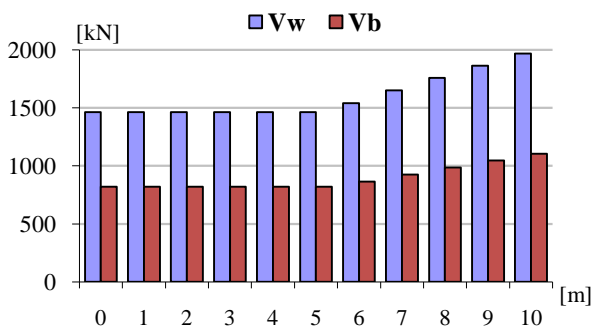

Fig. 19. Comparison of the base shears of tank wall and tank bottom as function of the tank fluid filling

The total base shear at the bottom of the wall consists of the sum V_i, V_c and V_w. The total base shear at below the tank base slab consist of the sum V_i, V_c, V_w and V_b too. Index i means a fluid impulsive component, index c a fluid convective component, index w a tank wall component and index b a tank bottom component.

Figures 20 and 21 show:
- comparison of the total base shears at the bottom

of the wall as function of the tank fluid filling, Fig. 20,
- comparison of the total base shears immediately at below the tank base slab as function of the tank fluid filling, Fig. 21.

The maximal value of total base shear above the tank bottom plate is for maximal fluid filling 10 m 5,852.97 kN and the total base shear below the tank bottom plate 6,957.45 kN.
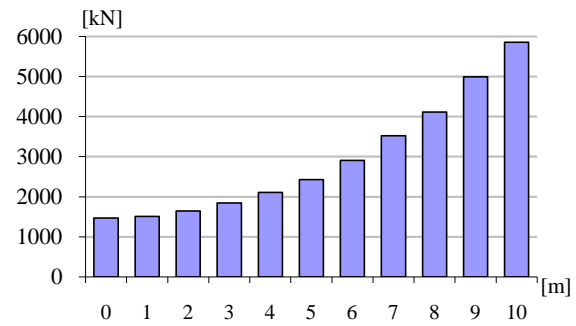

Fig. 20. Comparison of the total base shears V at the bottom of the wall as function of the tank fluid filling
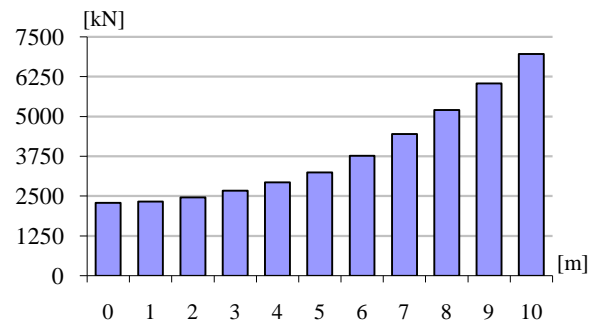

Fig. 21. Comparison of the total base shears $V*$ at below the tank as function of the tank fluid filling
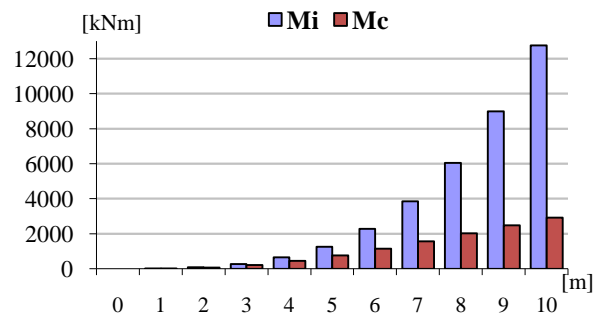

Fig. 22. Comparison of the bending moments immediately above the base plate in impulsive and convective mode of fluid as function of the tank fluid filling
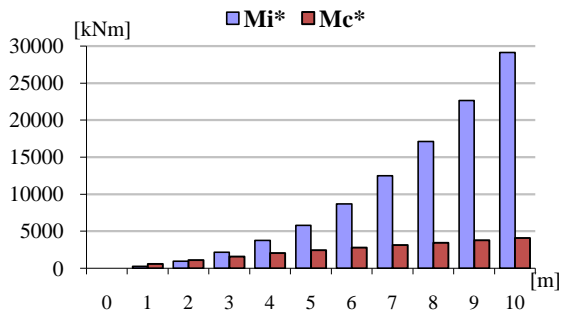
Fig. 23. Comparison of the bending moments immediately bellow the base plate in impulsive and convective mode of fluid as function of the tank fluid filling
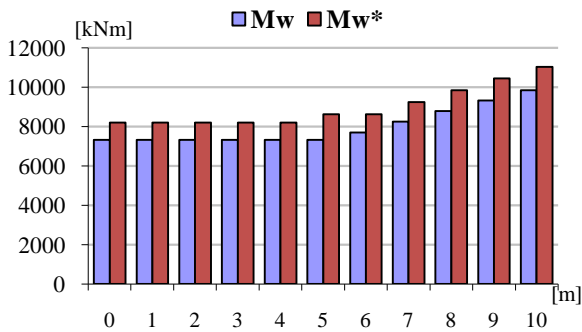

Fig. 24. Comparison of the bending and total overturning moments of tank wall as function of the tank fluid filling

Figure 22 shows comparison of the bending moments in impulsive and convective mode of fluid as function of the tank fluid filling and on the other side and comparison of the overturning moments in impulsive and convective mode of fluid is shown in Figure 23. It is seen that value of the bending and overturning moments in impulsive mode of fluid are grooving notable with height of tank fluid filling, respectively with the mass of fluid. We can see in Figure 24 the comparison of the bending and overturning moments of tank wall only as function of the tank fluid filling. On the increase of the total moments has decisive influence the moments in impulsive mode of fluid.

Figures 25 and 26 documents:
- comparison of the total bending moment immediately above the base plate as function of the tank fluid filling,
- comparison of the total overturning moment immediately bellow the base plate as function of the tank fluid filling.

The maximal value of total bending moment, i.e. the moment above the tank bottom plate is for

maximal fluid filling 10 m 25,523.26 kNm and the total overturning moment below the tank bottom plate 44,581.83 kNm.
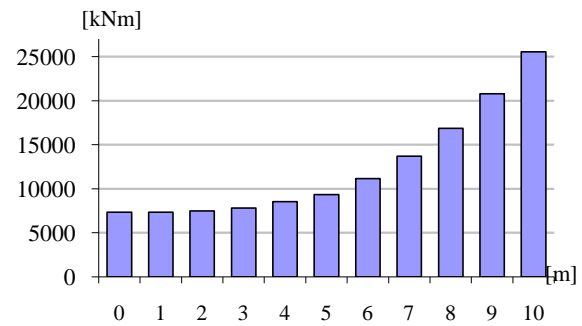

Fig. 25. Comparison of the total bending moment M immediately above the base plate as function of the tank fluid filling
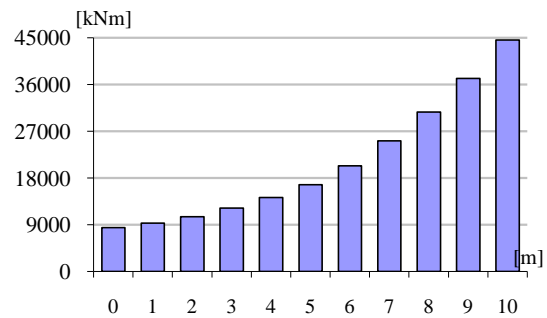

Fig. 26. Comparison of the total overturning moment M^* immediately bellow the base plate as function of the tank fluid filling
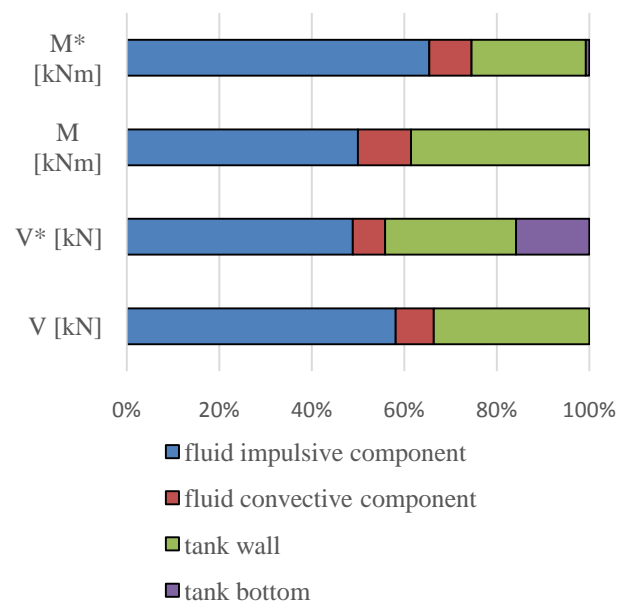

Fig. 27. Comparison of V, V^*, M, M^* components for full fluid filling tank

It is seen from Eq. (16) – (19) that we can receive the total base shears and the total moments by sum of these components: fluid impulsive component, fluid convective component, tank wall component, tank bottom component and tank roof component. Figure 27 presents component's part of the total base shears V at the bottom of the wall, the total base shears V^* at below the tank base slab, the total bending moment M immediately above the base plate and the total overturning moment M^* immediately bellow the base plate for the ground supported concrete cylindrical water full filling tank without roof construction with diameter $D = 20$ m and height $H = 10$ m. The tank bottom component doesn't rise by calculating of the total base shears V and the total bending moment M. The marked seismic effect were received from fluid impulsive component and tank wall component.

5 Conclusions

The seismic analysis of liquid storage containers is really highly complex problem. The knowledge of earthquake fluid effect on tank solid domain, forces acting onto containers, pressures in solid of tanks, surface sloshing process and maximal height of liquid wave during an earthquake is very important for dynamic analysis and seismic design of earthquake resistance structures - containers.

    This paper summarizes the results of analytical investigation of ground supported cylindrical tank partially and full fluid filling under horizontal earthquake ground motion using the elastic response spectrum for Slovakia $a_g = 1.5$ ms^{-2} for B category of subsoil. The basic responses were: base shears, bending and overturning moments as functions of the tank fluid filling. The ground supported concrete cylindrical tank without roof slab with capacity 3000 m^3 with inner radius $R = 10$ m and height H 10 m, is analysed in this study. The reservoir is filled to maximal height 10 m. We considered different height water filling of tank: 1 m, 2 m, 3 m, 4 m, 5 m, 6 m, 7 m, 8 m, 9 m, theoretically 10 m and empty tank too. The tank slenderness parameters $\gamma = H/R$ take values 0.1 - 1.0.

It is seen from results in chapter 4 that:
- the maximum values of seismic response liquid storage tank growth with tank full filling, with the amount of stored water, i.e. the mass of the liquid.
- the impulsive components of hydrodynamic effect obtain bigger values when thank is fuller, i.e. in narrow high (slender) tanks,
- the convective components of hydrodynamic effect receive bigger as impulsive effect when tank is emptier, i.e. in short, large-scale tanks,
- the total mass of fluid, the total base shear and the total bending and overturning moments are bigger when tank is full filling,
- the increase of the total base shears and total moments have a decisive influence the base shears and moments in impulsive mode of fluid, the ratio impulsive component of fluid masses obtains bigger values in narrow and slender tanks.

The knowledge of fluid effect on solid domain of tanks and their interdependence are under earthquake loading significant for safe and economic design of earthquake-resistant containers.

References:
[1] M. Farajian, M. I. Khodakarami, D.-P. N. Kontoni: Evaluation of soil-structure interaction on the seismic response of liquid storage tanks under earthquake ground motions. *Computation.* (MDPI, Demos T. Tsahalis), 2017, 5, 7, pp.1-12.
[2] A. Doğangün, R. Livaoğlu, A comparative study of the seismic analysis of rectangular tanks according to different codes. *The 14th World Conference on Earthquake Engineering* October 12-17, 2008, Beijing, China.
[3] S. H. Helou, Seismic Induced Forces on Rigid Water Storage Tanks. *Asian Journal of Engineering and Technology.* Vol. 02, Issue 04, August 2014, ISSN: 2321 – 2462.
[4] G. W. Housner, Dynamic pressures on accelerated fluid containers. Division of Engineering, California institute of technology, Pasadena California, 1955.
[5] N. Jendzelovsky, L. Balaz, Analysis of cylindrical tanks under the seismic load. *Key Engineering Materials.* Vol. 691 (2016), pp. 285-296 ISSN: 1013-9826.

[6] O. R. Jaiswal, D. C. Rai, S. K. Jain, Review of Seismic Codes on Liquid-Containing Tanks. DOI: 10.1193/1.2428341

[7] K. Kotrasova, E. Kormanikova, The study of seismic response on accelerated contained fluid. *Advances in Mathematical Physics*. Vol. 2017 (2017), pp. 1-9. - ISSN 1687-9139

[8] J. Králik, Safety assessment of the seismic resistance of nuclear power plant technology. *MATEC Web of Conferences*. 107 (2017), pp. 1-8.

[9] M. Krejsa, R. Cajka, Probabilistic reliability assessment using statistical analysis of structural monitoring. *SEMC 2016*, pp. 1872-1877 ISBN: 978-113802927-9.

[10] M. Krejsa, P. Janas, V. Krejsa, Software application of the DOProC method. *International Journal of Mathematics and Computers in Simulation* (2014) 8, ISSN 1998-0159, pp. 121-126.

[11] M. Major, K. Kuliński, I. Major: Thermal and Dynamic Numerical Analysis of a Prefabricated Wall Construction Composite Element Made of Concrete-polyurethane. *Procedia Engineering*. 190 (2017), pp. 231-236.

[12] P. K. Malhotra, T. Wenk, M., Wieland, Simple procedure for seismic analysis of liquid-Storage tanks. *Structural Engineering International*, (2000) 3, pp. 197-201.

[13] J. Melcer, M. Kúdelčíková: Frequency characteristics of a dynamical system at force excitation. *MATEC Web of Conferences*. 107 (2017), pp. 1-7.

[14] K. Meskouris, B. Holtschoppen, Ch. Butenweg, J. Rosin: Seismic analysis of liquid storage tanks. *2nd INQUA-IGCP-56*, Earthquake Geology, Greece, 2011, pp. 136-139.

[15] V. Michalcová, L. Lausová, I. Skotnicová, S. Pospíšil: Computational Simulations of the Thermally Stratified Atmospheric Boundary Layer above Hills. *Procedia Engineering*. 190 (2017), pp. 134-139.

[16] J., Michel, M. Mihalikova, Degradation of pipes properties in creep conditions. *Acta Metallurgica Slovaca* (2000) 2, pp. 108-115. ISSN 1335-1532.

[17] M. Močilan, M. Žmindák, P. Pecháč, P. Weis, CFD Simulation of hydraulic tank, *Procedia Engineering*, 192 920170, pp. 609-614, ISSN:1877-7058

[18] S. Mönkölä, On the Accuracy and Efficiency of Transient Spectral Element Models for Seismic Wave Problems. *Advances in Mathematical Physics*. Vol. 2016, article ID 9431583, 15 pages, 2016. doi:10.1155/2016/9431583.

[19] B. Taraba, Z Michalec, V. Michalcova, T. Blejchar, M Bojko, M Kozubkova. CFD simulations of the effect of wind on the spontaneous heating of coal stockpiles. *Fuel* (2014) 118, ISSN 0016-2361, pp. 107-112.

[20] K. Tvrdá: RSM Method in Probabilistic Analysis of the Foundation Plate. *Procedia Engineering*. 190 (2017): pp. 516-521.

[21] V. Valašková, G. Lajčáková: Mutual Comparison of Two Pavement Computing Models. *Procedia Engineering*. 190 (2017), pp. 547-553.

[22] M. Zmindak, I. Grajciar, Simulation of the aquaplane problem. *Computers and Structures* (1977) 64, Issue 5-6, pp. 1155-1164.

[23] Eurocode 8 - Design of structure for earthquake resistance - Part. 4: Silos, tanks and pipelines. Januar 2006.

[24] IITK-GSDMA Guidelines for seismic design of liquid storage tanks - provisions with commentary and explanatory examples. Kanpur, Indian Institute of Technology Kanpur, 2005.